Geochemical Tracers in Earth System Science: Nitrogen Isotopes in Deep Time

SCHOLARONE™
Manuscripts

1   **Geochemical Tracers in Earth System Science: Nitrogen Isotopes in Deep Time**

2   Colin Mettam[1] and Aubrey L. Zerkle[2*]

3   [1]Department of Earth Sciences, University College London

4   [2]School of Earth & Environmental Sciences and Centre for Exoplanet Science, University of St
5   Andrews

6   *corresponding author: az29@st-andrews.ac.uk

7

8   **Abstract**

9   Nitrogen is an essential nutrient for life, and its sources and cycling have varied over Earth history.
10   Stable isotope ratios of nitrogen compounds (expressed as $\delta^{15}N$, in ‰) are preserved in the
11   sedimentary record and track these changes, providing important insights into associated
12   biogeochemical feedbacks. Here we review the use of nitrogen stable isotope geochemistry in
13   unravelling the evolution of the global N cycle in deep time. We highlight difficulties with
14   preservation, unambiguous interpretations, and local versus global effects. We end with several case
15   studies illustrating how depositional and stratigraphic context is crucial in reliably interpreting $\delta^{15}N$
16   records in ancient marine sediments, both in ancient anoxic (Archean) and more recent well
17   oxygenated (Phanerozoic) environments.

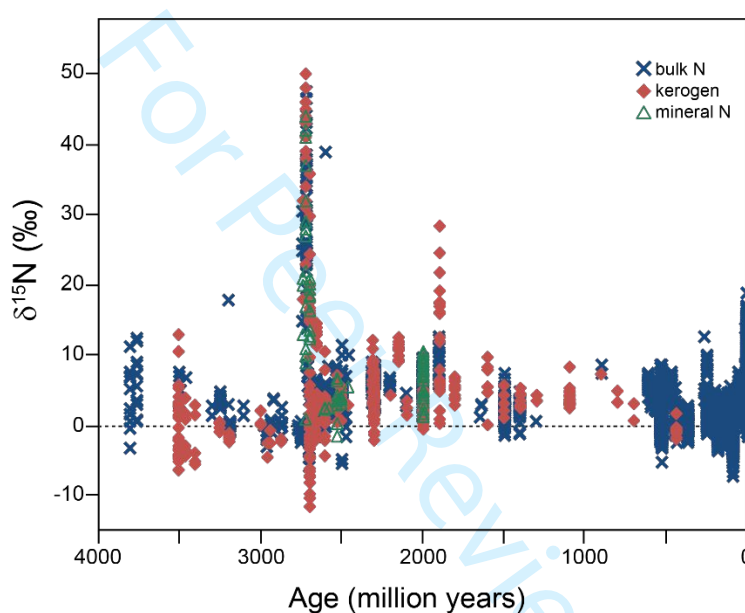18   **1. Introduction – Nitrogen in Life**

19   Nitrogen (N) is an essential nutrient for life, as it is critical in the formation of biomolecules,
20   including nucleic acids and proteins. Despite an abundant reservoir of N_2 in the atmosphere, only a
21   limited number of micro-organisms (nitrogen-fixing organisms, or "diazotrophs") have evolved the
22   ability to directly assimilate di-nitrogen. All other organisms rely either on ammonium (NH_4^+) or
23   ammonia (NH_3) released during the remineralization of biomass, or on the products of oxidized
24   ammonium/ammonia generated by biologically mediated transformations in the nitrogen cycle, such
25   as nitrate (NO_3^-) and nitrite (NO_2^-).

26   Deciphering the evolution of the nitrogen cycle through geological time and the relative abundances
27   of different bioavailable nitrogen compounds is therefore critical to understanding the emergence and
28   radiation of early life, and to elucidating key biological and environmental transitions in the
29   Phanerozoic. Such changes can be tracked by measuring the two stable isotopes of nitrogen in Earth
30   materials (^{14}N and ^{15}N – expressed as $\delta^{15}N$ in ‰, and described below), since different nitrogen
31   cycling reactions express different isotopic fractionations in $\delta^{15}N$. The resulting N isotope ratios are
32   reflected in biomass, which in turn can be archived in the sedimentary record (e.g., as reviewed in
33   Stüeken et al., 2016) (Figure 1).

34   A seminal paper analysing changes in the marine nitrogen cycle through the Precambrian from
35   temporal $\delta^{15}N$ trends was published by Beaumont and Robert (Beaumont and Robert, 1999). These
36   authors found a shift from $\delta^{15}N$ values in kerogen centered around 0‰ in the Archaean, to positive
37   $\delta^{15}N$ values centered around +5‰ from the Paleoproterozoic onwards. They suggested that these
38   records were broadly indicative of an anaerobic NH_4^+-based nitrogen cycle in the Archean, giving
39   way to an aerobic nitrogen cycle with available nitrite and nitrate after the Great Oxidation Event
40   (GOE). In the ensuing two decades, the $\delta^{15}N$ proxy has become increasingly utilized for
41   paleoenvironmental and paleoredox studies in deep time (here defined as pre-Cenozoic; e.g., Ader et
42   al., 2016; Stüeken et al., 2016a), with more recent targeted studies largely supporting these broad
43   temporal trends (e.g., Kipp et al., 2018; Yang et al., 2019; Zerkle et al., 2017).

44   Notwithstanding the general step-wise expansion of aerobic nitrogen cycling, nitrogen isotope studies
45   of sediments spanning Earth's history have revealed spatial and temporal nuances within this
46   narrative. For example, some δ^{15}N trends in Late Archean sediments have been interpreted to
47   represent periods of temporally and spatially constrained aerobic N cycling prior to the GOE (Garvin
48   et al., 2009; Godfrey and Falkowski, 2009; Yang et al., 2019; Mettam et al., 2019). More recent δ^{15}N
49   records have identified periods of time when anaerobic nitrogen cycling dominated in the
50   Phanerozoic, including during the Latest Permian Extinction Event (LPEE; e.g., Saitoh et al., 2014)
51   and Cretaceous Ocean Anoxic Events (OAEs; e.g., Junium and Arthur, 2007).

52   Interpretations of these records, and the biogeochemical feedbacks they imply, critically rely on the
53   ability of sedimentary δ^{15}N to reliably record the isotopic fingerprints of the coeval marine nitrogen
54   cycle. Here we discuss the state of the field in low-temperature N isotope biogeochemistry, including
55   susceptibility to syn- and post-depositional alteration, ambiguities with respect to interpretations, and
56   local versus global effects. Notably, we argue that stratigraphic and depositional context is crucial in
57   reliably interpreting nitrogen stable isotope records in ancient marine sediments.

58

59   **Figure 1.** Temporal trends in δ^{15}N over Earth history, as preserved in the sedimentary rock record (updated
60   from Yang et al., 2019, and references therein).

61

62   **2. The δ^{15}N Proxy in a Nutshell**

63   Multiple biologically mediated redox transitions occur between nitrogen-containing compounds in the
64   marine N cycle. These transitions and their associated δ^{15}N fractionations are summarised in Figure 2.
65   The δ^{15}N values of nitrogen compounds are expressed relative to the isotopic composition of
66   atmospheric nitrogen, using the standard delta notation:

67   δ^{15}N (‰) = ((^{15}N/^{14}N)$_{sample}$ /(^{15}N/^{14}N)$_{air}$ − 1) x 1000,

68   with isotopic fractionations for specific reactions shown as $\varepsilon \approx \delta^{15}N_{product} - \delta^{15}N_{reactant}$.

69   N$_2$ fixation is the primary source of nitrogen input into the marine system and is regulated by the
70   availability of phosphorous and micro-nutrients, such as Mo and Fe (e.g., Zerkle et al., 2006).
71   Diazotrophs incorporate nitrogen into their biomass directly from atmospheric or dissolved N$_2$.
72   Remineralization of this biomass in the water column and in sediments releases bioavailable
73   ammonium or ammonia, which can in turn be assimilated by non-diazotrophic organisms. N$_2$ fixation
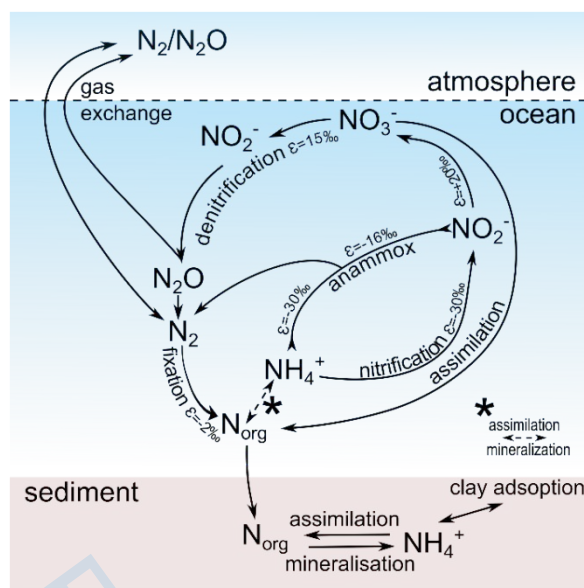
2

74   and the recycling of NH_4^+ generally impart only small fractionations in $\delta^{15}N$ ($\varepsilon \leq 2‰$). Therefore, in
75   an environment where N_2 fixation and the recycling of NH_4^+ are the dominant N sources, the $\delta^{15}N$ of
76   biomass broadly reflects the atmospheric input value ($\delta^{15}N \approx 0‰ \pm 2‰$). However, if NH_4^+ or other
77   forms of dissolved inorganic nitrogen (DIN) are readily available, diazotrophy will be suppressed, as
78   N_2 fixation is energetically expensive in comparison to assimilation.

79   In the presence of oxygen, ammonium/ammonia undergoes microbially-mediated sequential oxidation
80   to nitrite (NO_2^-) and nitrate (NO_3^-). In modern oxygen-rich settings this biological nitrification process
81   is rapid and quantitative, making NO_3^- the largest reservoir of bioavailable DIN in the oceans.
82   Although nitrification can produce large fractionations in $\delta^{15}N$, the quantitative nature of NH_4^+
83   oxidation in the modern oceans means that these isotopic fractionations are suppressed in the resultant
84   nitrate pool.

85   Nitrate and nitrite both form important sources of nutrient N in modern oceanic settings; however,
86   they can also be utilized as electron acceptors in chemotrophic metabolisms. Nitrate can be reduced to
87   N_2 during heterotrophic denitrification, a form of anaerobic respiration of organic carbon with NO_3^-,
88   which is second only to aerobic respiration in reduction potential. This canonical form of
89   denitrification proceeds through NO_2^- and a number of intermediate N phases that can also build up in
90   the environment (e.g., N_2O). Nitrate reduction can further be coupled to the oxidation of reduced
91   compounds like sulfide, methane, or hydrogen during chemoautotrophy. Nitrate reduction can also
92   proceed via dissimilatory reduction to ammonium (DNRA), which provides a competitive advantage
93   under nitrate-limiting conditions since it requires less nitrate per mole of organic substrate. Finally,
94   some organisms can utilize nitrite to oxidize NH_4^+ during anaerobic ammonium oxidation
95   (anammox). The reduction of NO_3^-/NO_2^- to N_2 during denitrification and anammox can have
96   important implications for the oceanic nitrogen budget, as these processes remove bioavailable
97   nitrogen from the oceanic reservoir. In the case of DIN loss, and if other nutrients remain available,
98   diazotrophs will have a competitive advantage, and can proliferate to restore the balance of fixed N to
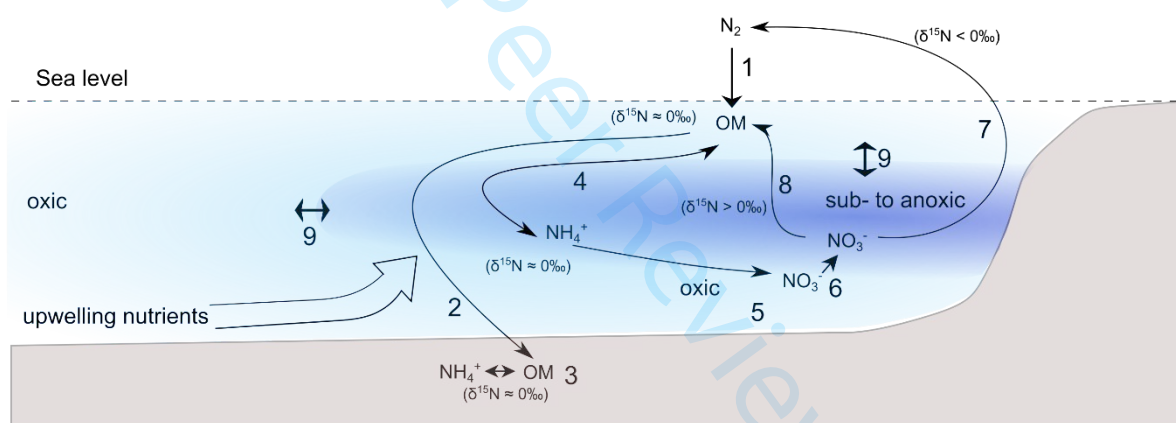99   the marine system. (e.g., Megonigal et al., 2003; Voss et al., 2012).

100   These N loss processes can all produce large fractionations in $\delta^{15}N$ ($\varepsilon = +20$ to $+30‰$; Brunner et al.,
101   2013; Granger et al., 2008). In marine sediments denitrification is generally quantitative such that no
102   fractionations are expressed. However, in the water column, denitrification is constrained to low-
103   oxygen settings such as oxygen minimum zones (OMZs; Figure 3.). This results in incomplete
104   denitrification in the water column, leaving a residual pool of NO_3^- that carries a positive $\delta^{15}N$ value.
105   Anammox produces a similar fractionation effect for $\delta^{15}N$, but its role in the global N cycle and in the
106   N isotope budget is somewhat less well-constrained and the relative contributions of anammox and
107   canonical denitrification remain an area of active research.

108   The balance between N_2 fixation and the assimilation of NO_3^- carrying the positive $\delta^{15}N$ signature of
109   denitrification/anammox controls the $\delta^{15}N$ values of modern marine biomass. Today, aerobic N loss
110   processes produce organic matter with an average $\delta^{15}N$ of $\sim+6‰$ (Peters et al., 1978). However, the
111   $\delta^{15}N$ of particulate organic matter and underlying sediments is spatially and temporally
112   heterogeneous, following subtle redox and productivity variations in the modern marine system (e.g.,
113   De Pol-Holz et al., 2009). In addition, changes in the redox state and nutrient dynamics of marine
114   settings over Earth's history have seemingly allowed for unique configurations of the nitrogen cycle
115   that produce both highly positive and highly negative $\delta^{15}N$ values not seen on Earth today (Figure 1).
116   We explore some of these records, and their potential (largely non-unique) interpretations in the case
117   studies below.

118

119   **Figure 2.** Major transformations in the marine nitrogen cycle, showing average values for fractionations
120   (adapted from Granger et al., 2008, Ader et al., 2016, and references therein). Fractionations not specifically
121   shown (e.g., for assimilation and mineralization), are generally 0‰.

122

123   **Figure 3.** Nitrogen cycling in a Phanerozoic Oxygen Minimum Zone (OMZ) (adapted from Pinti and
124   Hashizume, 2011). (1) Fixation of gaseous nitrogen (N_2) into biomass (organic matter, OM) by diazotrophs; (2)
125   transport of OM to the sediments, i.e., via the biologic pump; (3) OM can be preserved in the sediments or
126   remineralized to NH_4^+, which can then be reassimilated into OM by benthic organisms or adsorbed onto clay
127   minerals; (4) Remineralization of OM to NH_4^+ and reassimilation of NH_4^+ in low-oxygen settings; (5) in oxic
128   settings NH_4^+ is oxidised to NO_2^- and NO_3^-; (6) upwelling of NO_3^- into low-oxygen setting; (7) partial
129   denitrification of NO_3^- (and reduction of NO_2^- by anammox) in sub- to anoxic settings releases N_2 to
130   atmosphere. Partial denitrification renders the residual pool of NO_3^- isotopically heavy (+ $\delta^{15}N$); (8) assimilation
131   of this residual pool of NO_3^- contributes to the positive $\delta^{15}N$ values of Phanerozoic OM; (9) the size of OMZs
132   can expand and contract enhancing or reducing denitrification and the resulting N isotope effects.

133

134   **3. Methods and Limitations**

135   Nitrogen isotopes are now routinely measured alongside carbon isotopes in sedimentary rocks. Most
136   recent studies have measured sedimentary $\delta^{15}N$ using an elemental analyser coupled to an isotope
137   ratio mass spectrometer running in continuous flow mode (CF-EA-IRMS). This method is more
138   widely accessible and significantly less time consuming than previously developed offline methods

4

139   (see Ader et al., 2016, for a comprehensive review). The CF-EA-IRMS method generally works well
140   for sediments with high N contents (1σ of ± 0.25‰ for N > 700ppm; Bahlmann et al., 2010).
141   However, the low N content and high TOC/TN ratios in most Precambrian rocks can lead to some
142   analytical challenges. In this case, additional steps are required to correct for blanks and ensure
143   complete combustion to prevent isobaric interferences, e.g., with CO (Beaumont et al., 1994).

144   Several new methods have been developed in the past decade that also allow for accurate $\delta^{15}N$
145   measurements on samples with much lower abundances of N. The nano-EA-IRMS method (Polissar
146   et al., 2009) uses a custom cryo-trap and chromatography system to concentrate the evolved N_2 gas
147   before analysis, decreasing the sample size requirements by several orders of magnitude. This method
148   has been successfully applied to analyze $\delta^{15}N$ values in deep time sediments (e.g., Mettam et al.,
149   2019; Yang et al., 2019), but blanks remain an issue and must be closely monitored and corrected for.
150   Alternatively, samples can be run in triplicates of varying mass. These triplicates can then be plotted
151   on 'Keeling' plots, with the true value calculated as the intercept with the y-axis (see Mettam et al.,
152   2019). An off-line tube cracker combustion system has also been successfully applied as an
153   introduction system to the CF-EA-IRMS to measure $\delta^{15}N$ in low N abundance sediments (e.g.,
154   Stüeken et al., 2015a), but requires very high vacuum. Ishida et al. (2018) recently described a method
155   for measuring $\delta^{15}N$ values in organic matter *in situ* using secondary ion mass spectrometry (SIMS),
156   with analytical precision on the same order as bulk methods (2σ of ± 0.56‰). Spatially resolved $\delta^{15}N$
157   analyses should be useful in discerning $\delta^{15}N$ at the single cell or organismal level (e.g., with
158   Precambrian microfossils); however, the SIMS technique measures $\delta^{15}N$ on the CN⁻ ion, so cannot be
159   used to measure mineral NH_4^+, e.g., in clay minerals that don't contain carbon.

160   Despite a recent upswing in the use of $\delta^{15}N$ values in deep time paleoenvironmental and paleoredox
161   studies, post-depositional alteration remains an issue, and the relative ability of different sedimentary
162   N phases to resist alteration is hotly debated. In the following sections we discuss post-depositional
163   alteration of N stable isotope ratios, and the consensus (or lack thereof) for which N phases most
164   faithfully retain their original $\delta^{15}N$ signatures.

165   *3.1 The Problem with Preservation*

166   In order to reconstruct ancient nitrogen cycling from the sedimentary rock record, the organic matter
167   preserved within these sediments must faithfully record the $\delta^{15}N$ values of the coeval marine biomass.
168   Post-mortem, marine phytoplankton will sink to the sea floor, aided by the biological pump (at least in
169   the Phanerozoic). Some of this organic matter will be remineralized in the water column or directly
170   consumed on descent, which could affect $\delta^{15}N$ values. Modern N isotope studies have shown that the
171   oxidation of sinking particulate matter can be an important consideration for preservation, as
172   deamination of organic matter can selectively liberate ^{15}N-depleted ammonium, thereby slightly
173   increasing the residual $\delta^{15}N$ values (Möbius et al., 2010).

174   Primary N isotope values can be further modified by syn- and post-depositional processes in the
175   sediments, including diagenesis, metamorphism, and hydrothermal or hydrocarbon fluid migration.
176   Numerous theoretical and empirical studies have been utilized to estimate these effects (e.g., see
177   review in Ader et al., 2016). While the detailed findings of these studies differ, the processes that
178   seem to impart the largest changes in the primary $\delta^{15}N$ values include aerobic degradation of organic
179   matter during early diagenesis, which can increase $\delta^{15}N$ values by 2-4‰ (Freudenthal et al., 2001),
180   and high-temperature metamorphism above greenschist facies, which can increase $\delta^{15}N$ values by up
181   to 5‰ (Bebout and Fogel, 1992; Boyd and Philippot, 1998).

182   Nitrogen isotope values can be modified by syn-depositional degradation of organic matter within the
183   sediments, either by aerobic or anaerobic respiration (e.g., sulphate reduction) (Altabet and Francois,
184   1994; Macko and Estep, 1984). However, these ^{15}N-enrichments can be muted if the evolved NH_4^+ is
185   quantitatively reincorporated into new benthic biomass or adsorbed onto clay mineral phases

                                                                                                          5

186   (Robinson et al., 2012). Potential loss of nitrogen during degradation can be qualitatively assessed by
187   examining the ratios of organic carbon to total nitrogen (C/N ratios) in the sediments. The Redfield
188   ratio for pristine marine phytoplankton is between ~4 and ~8 (Gao et al., 2012; Meyers, 1997).
189   Sedimentary values below this lower threshold would indicate that a significant amount of carbon was
190   lost during degradation, while liberated NH_4^+ was largely captured and retained on clay surfaces.
191   These considerations are complicated for many Precambrian sediments, where C/N ratios are
192   extremely high (> 100). In addition, the use of C/N ratios to infer preservation in Phanerozoic
193   sediments can be complicated by mixing with terrestrial vegetation, which has a higher C/N ratio of >
194   ~15 (Gao et al., 2012; Meyers, 1997); such mixed provenance can potentially be untangled by coeval
195   biomarker analyses, as discussed below.

196   Modification of sedimentary $\delta^{15}N$ values by metamorphism is particularly well-documented, and
197   generally increases with metamorphic grade. Thermal alteration results in the preferential liberation of
198   the lighter stable isotope, which increases $\delta^{15}N$ and $\delta^{13}C$ values. These effects can be identified by a
199   diagnostic positive correlation between $\delta^{15}N$ and $\delta^{13}C$, and by negative correlations between total
200   nitrogen (TN) and $\delta^{15}N$, or organic carbon (TOC) and $\delta^{13}C$. Stüeken et al. (2017) further proposed that
201   C/H ratios in kerogen can be used as a proxy for thermal alteration in metamorphosed sediments.
202   Regardless, metamorphic effects on $\delta^{15}N$ are generally mild (1-2‰) at greenschist facies or below,
203   thus the majority of sedimentary $\delta^{15}N$ studies have focused on low metamorphic grade sediments.

204   *3.2 The $\delta^{15}N_{org}$ versus $\delta^{15}N_{bulk}$ Debate*

205   Issues surrounding post-burial preservation and alteration are also intrinsic to the debate over whether
206   $\delta^{15}N$ values in bulk sediments ($\delta^{15}N_{bulk}$) or in extracted organics ($\delta^{15}N_{org}$) are a more reliable recorder
207   of sedimentary organic nitrogen. The former includes a combination of nitrogen contained in organic
208   matter and NH_4^+ adsorbed onto clay minerals or substituted into minerals as a replacement for
209   potassium (K^+), while the latter represents the acid-resistant organic fraction. This debate stems from
210   discrepancies between $\delta^{15}N_{bulk}$ and $\delta^{15}N_{org}$ values, which often show an offset between isotopically
211   lighter $\delta^{15}N_{org}$ and heavier $\delta^{15}N_{bulk}$ within the same sample.

212   Proponents of analyzing sedimentary organic matter (or kerogen) argue that this archive is less easily
213   altered or exchangeable than more mobile N pools, such as clay-sorbed NH_4^+. However, concerns
214   remain about the efficiency and selectivity of specific methods for kerogen extraction. Most kerogen
215   extraction techniques use a series of rock powder dissolutions with increasingly corrosive acids to
216   dissolve the carbonate and silicate fractions (often HCl-HF). Notably, recalcitrant minerals that are
217   also resistant to HF digestion, such as pyrite, can be retained through these extraction procedures.
218   While these minerals do not generally contain N, they do influence the nitrogen abundance values of
219   kerogen (total organic nitrogen, TON wt. %), complicating interpretations of TON. These minerals
220   can be removed by the inclusion of a heavy mineral separation step after acid digestion, e.g., with
221   chloroform. A greater concern is the formation of neo-minerals, such as fluoride salts, which can alter
222   measured $\delta^{15}N$ values during the combustion of samples in EA-IRMS. The formation of calcium
223   fluoride (CaF) can be prevented to some extent by digestion of sediments in HCl and thorough rinsing
224   to remove carbonate-associated Ca^{2+} prior to HF extraction; however, this remains an issue for
225   samples with high abundances of Ca-bearing silicates. An additional digestion using a combination of
226   HF and boric acid to produce BF_3 has recently proven effective in removing secondary fluorides
227   (Stüeken et al., 2017).

228   Proponents of analysing bulk sediments suggest that the offset between $\delta^{15}N_{org}$ and $\delta^{15}N_{bulk}$ from the
229   same sample indicates that significant amounts of ^{15}N must have been liberated from kerogen and
230   ultimately captured on clays. Recent work by Stüeken et al. (2017) suggested that metamorphism
231   drives organic $\delta^{15}N$ values lighter and silicate-bound $\delta^{15}N$ values heavier, resulting in a 3-4‰ offset at
232   greenschist facies or lower. However, the mechanism(s) behind this offset remain unclear. If this
233   difference occurs when NH_4^+ is transferred from kerogen to clays during early diagenesis, it could

6

234 result from the preferential removal of isotopically heavy protein-derived organic matter from
235 kerogen or the preferential preservation of isotopically light porphyrins in the kerogen; if it occurs
236 during thermal maturation, it could be caused by changes in bonding as kerogen matures and clays
237 dewater (Stüeken et al., 2017).

238 These arguments imply that $\delta^{15}N_{bulk}$ could provide the most reliable sedimentary archive, particularly
239 when the majority of nitrogen resides in silicates phases. However, the retention of primary $\delta^{15}N$
240 values in bulk sediments require that post-depositional processes occur within a closed-system that
241 captures most of the NH_4^+ evolved from organic matter (e.g. Robinson et al., 2012). In addition,
242 $\delta^{15}N_{bulk}$ data is susceptible to overprinting and isotope exchange between clay-bound NH_4^+ and NH_4^+
243 from migrating metasomatic fluids. Kump et al. (2011) suggested that potential overwriting by
244 metasomatic NH_4^+ should be identifiable by strong correlations between TN, $\delta^{15}N_{bulk}$ and potassium
245 (K, wt%), given the abundance of K in metasomatic fluids. Similar correlations should also identify
246 contamination by allochthonous clay-associated NH_4^+ brought to the depocenter from eroding
247 hinterlands, although such contamination with exogenous N is less easily identified. Given the
248 propensity for these post-depositional processes to alter different N phases, and the lack of a
249 consensus from the community as to which record is more reliable, many studies now report both
250 $\delta^{15}N_{bulk}$ and $\delta^{15}N_{org}$ data, and comparison of these two datasets can reveal further insights into data
251 fidelity (e.g., Koehler et al., 2018; Yang et al., 2019).

252

253 **4. Case Studies**

254 Taking into account the precautions discussed above, $\delta^{15}N$ values provide important insights into past
255 biogeochemical nitrogen cycling in well-preserved sedimentary rocks. Reliable $\delta^{15}N$ data have been
256 generated in sediments as old as 3.8 Ga (Papineau et al., 2005), and provide an interesting narrative of
257 marine nutrient cycling following from biological revolutions that occurred over Earth history. Even
258 the earliest $\delta^{15}N$ records show evidence for N_2 fixation (Stüeken et al., 2015a) consistent with
259 phylogenetic suggestions that diazotrophy arose very early in life's history (Weiss et al., 2016). As
260 discussed above, the long-term narrative of nitrogen cycling through geological time documents a
261 change from dominantly anaerobic to aerobic N-cycling, consistent with the progressive oxygenation
262 of the biosphere. However, recently published records hint at earlier spatial and temporal
263 heterogeneities, even in a largely anoxic Late Archean world. In addition, records of $\delta^{15}N$ are
264 increasingly being utilized to examine the role of nutrients in more recent transitions in Earth history,
265 including mass extinction events in the Phanerozoic. Here we present three case studies illustrating
266 the utility and complexity of the $\delta^{15}N$ proxy in deciphering the biogeochemical nitrogen cycling in the
267 Late Archean and Late Permian marine systems.

268 *4.1 Extreme $\delta^{15}N$ values at ~2.7 Ga – marine versus terrestrial signals?*

269 Both extremely high and extremely low $\delta^{15}N$ values have been measured in sediments from ~2.7 Ga
270 (Figure 1), and variably linked to global oxygenation and primary production. $\delta^{15}N$ values as high as
271 +50‰ in the Tumbiana Formation (Fortescue Group, Western Australia) have been interpreted to
272 represent partial nitrification under conditions where ammonium was abundant and oxygen was
273 limited (Thomazo et al., 2011). This interpretation stems largely from laboratory incubations with
274 methanotrophic bacteria that produced extremely ^{15}N-depleted N_2O (-46‰) during the co-oxidization
275 of ammonium with methane (Mandernack et al., 2009). The co-occurrence of these large $\delta^{15}N$ values
276 with very low $\delta^{13}C_{org}$ values in the Tumbiana Formation supports the incorporation of methane into
277 these sediments. However, this interpretation remains problematic for several reasons (e.g., Stüeken et
278 al., 2015b). Namely, in order for isotopic fractionations this large to be expressed in the residual
279 NH_4^+, a large fraction of the available ammonium (> 70%) would have had to be oxidized. The
280 residual ammonium would still have been assimilated into biomass, while the resulting NO_2^- and NO_3^-

281 would have been respired. Similarly, in order for the high $\delta^{15}N$ values to have been preserved in the
282 resulting organic matter, the product NO_2^- would have to be lost from the system (e.g., via
283 denitrification and/or anammox) rather than re-assimilated. Stüeken et al. (2015b) alternatively
284 suggested that the Tumbiana Formation and underlying Kylena Formation represent a lake system that
285 was driven highly alkaline by aqueous alteration of underlying volcanics. In an anoxic alkaline lake
286 setting, the volatilization of NH_4^+ to ammonia (NH_3) could produce large N isotope fractionations,
287 similar to high $\delta^{15}N$ values in alkaline lakes today.

288 Extremely low $\delta^{15}N$ values have recently been reported from ~2.7 Ga sediments of the Manjeri
289 Formation (Belingwe Greenstone Belt, Zimbabwe) (Yang et al., 2019). These values, down to -11‰,
290 were interpreted to form from incomplete assimilation of a non-limiting pool of upwelling NH_4^+. This
291 scenario was linked to a rise in global primary productivity following the expansion of oxygenic
292 photosynthesis. The associated surge in primary productivity could have enhanced organic matter
293 export and remineralization, leading to the accumulation of NH_4^+ in anoxic deep waters. This pool of
294 NH_4^+ could have been upwelled into highly productive surface oceans and partially assimilated by
295 primary producers preferentially utilizing isotopically light NH_4^+. In addition, uptake of light NH_4^+
296 would have left the residual pool of DIN isotopically heavy. Assimilation of this residual pool of
297 isotopically heavy NH_4^+, either separated in time or space, could also have contributed to production
298 of positive $\delta^{15}N$ values in the Late Archean (Ader et al., 2016; Yang et al., 2019).

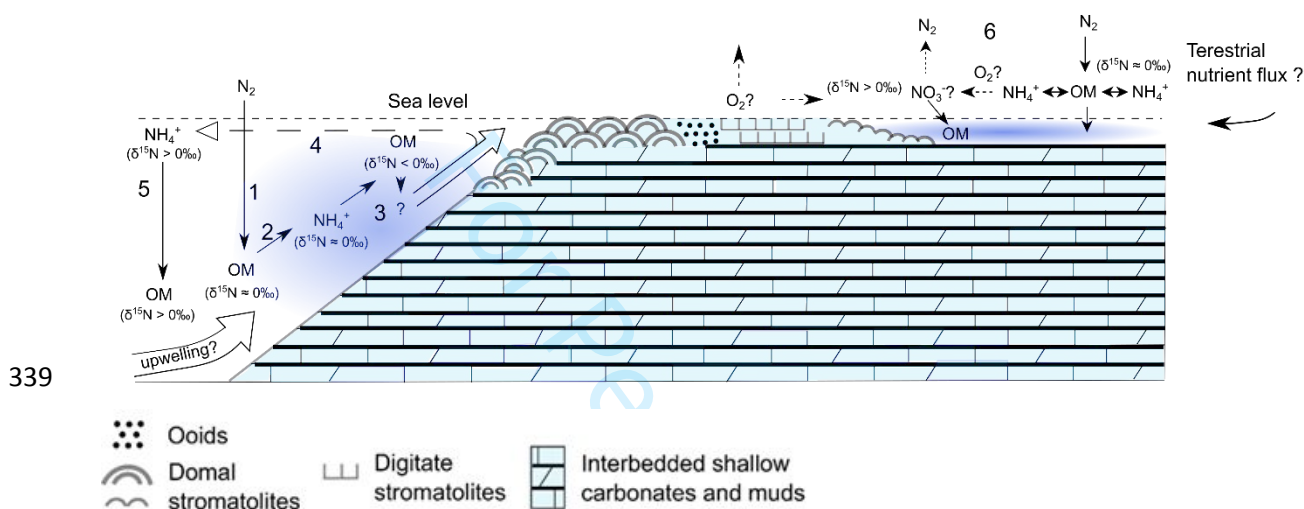299 *4.2 Pre-GOE positive $\delta^{15}N$ values - alternatives to oxygen?*

300 Despite the general narrative of an anaerobic Archean N cycle giving way to aerobic N cycling
301 sometime later in Earth history, the exact timing of this transition is debated. Some statistical
302 treatments of the secular $\delta^{15}N$ record seem to imply that nitrate was widely available by ~2.5 Ga
303 (Stüeken et al., 2016), while others suggest that a turning point in the N cycle occurred in association
304 with the GOE at ~2.3 Ga (Zerkle et al., 2017). Positive $\delta^{15}N$ values in Late Archean sediments have
305 also been interpreted to imply the early onset of aerobic N cycling; however, these data are not
306 without controversy, and lend themselves to alternative interpretations.

307 Small increases in $\delta^{15}N$ values preserved within ~2.5 Ga sediments from the Mt McRae Formation in
308 Western Australia (Garvin et al., 2009) and the Ghaap Group in South Africa (Godfrey and
309 Falkowski, 2009) have been suggested to record the transient or localized appearance of nitrification
310 and denitrification in association with "whiffs" of oxygen in the marine environment. However, these
311 sediments were deposited in distal and relatively deep waters, separated from oxygen oases in
312 shallow, highly productive shelf environments where oxygen production was most likely to have
313 occurred (e.g., Olsen et al., 2013). Therefore, these sediments could instead represent nitrogen redox
314 cycling in open ocean or deeper water environments independent of surface oxygen. For example,
315 positive $\delta^{15}N$ values preserved in ~2.5 Ga BIFs have been interpreted to reflect the assimilation of
316 NH_4^+ enriched in ^{15}N by partial oxidation to nitrite. However, these researchers argued that
317 ammonium oxidation could have been driven anaerobically by microbes utilizing Fe(III)-
318 oxyhydroxides formed in the water column, rather than by O_2 (Busigny et al., 2013).

319 $\delta^{15}N$ values of ammonium in the Late Archean could also have been driven higher by partial
320 assimilation, as described for ~2.7 Ga sediments above (Ader et al., 2016). Until recently this
321 interpretation was largely dismissed due to a lack of evidence for a correlative pool of ^{15}N-depleted
322 biomass. However, recent analyses of ~2.5 Ga rocks have identified comparatively low $\delta^{15}N$ values ($\leq$
323 -4‰) in shore-proximal sediments (Mettam et al., 2019). Combined with the ~2.7 Ga data (Yang et
324 al., 2019), these studies suggest that partial NH_4^+ assimilation could have been widespread once
325 oxygenic photosynthesis kick-started primary productivity in the Late Archean. These data
326 additionally illustrate the potential for spatial and temporal heterogeneity within the global marine N
327 cycle.

328   The study by Mettam et al. (2019) further demonstrates how depositional setting can play a key role
329   in spatially partitioning the nitrogen cycle, producing local variations in $\delta^{15}N$ values . For example,
330     $\delta^{15}N$ values of -4‰ were measured in sediments deposited from relatively deep shelf conditions,
331   where partial assimilation from a pool of upwelling NH_4^+ from the open ocean could have occurred.
332   In contrast, sediments deposited in shallower, more restricted lagoonal conditions retained $\delta^{15}N$ values
333   of ~0‰, likely reflecting diazotrophy and the efficient recycling of remineralized NH_4^+. Only a
334   handful of positive $\delta^{15}N$ values greater than 2‰ were reported from the same section, hinting at the
335   possible presence of coupled nitrification and incomplete denitrification (Figure 4). However, these
336   positive values were from shallow-water, carbonate-rich facies, probably indicating very localised
337   oxygenated settings. This spatial complexity highlights the importance of sedimentological and
338   depositional context for understanding local variations in $\delta^{15}N$ data.

339

340

Figure 4. Proposed nitrogen cycle in the Late Archean (adapted from Mettam et al., 2019). Nitrogen cycling
was likely spatially heterogenous, as follows: (1) N_2 fixation in the open ocean and transport of diazotrophic
biomass to the seafloor; (2) remineralization of OM to NH_4^+ and shoreward transport; (3) incomplete NH_4^+
assimilation, producing OM with negative $\delta^{15}N$ values; (4) transport of the residual NH_4^+ pool (left with positive
$\delta^{15}N$ values); and, (5) complete assimilation of NH_4^+ in the open ocean, producing OM with positive $\delta^{15}N$
values. (6) In a relatively restricted lagoonal environment isolated from marine influence these processes could
alternatively go to completion, such that the $\delta^{15}N$ of OM would reflect the input (0‰). Alternatively, if oxygen
oases are present, coupled nitrification/dentrification could produce OM with positive $\delta^{15}N$ values.

349

350   *4.2 The Late Permian Extinction Event – multiple controls on $\delta^{15}N$?*

351   Trends in Phanerozoic $\delta^{15}N$ values have also been utilized to examine changes in redox and nutrient
352   feedbacks during more recent events in Earth history. For example, nutrient stress during the Late
353   Permian has been implicated in contributing to the greatest extinction event in the Phanerozoic.
354   Notably, $\delta^{15}N$ values near 0‰ in palaeoequatorial Tethyan seas during the LPEE have been
355   interpreted to reflect enhanced denitrification and a proliferation of diazotrophy resulting from NO_3^-
356   limitation (as reviewed by Saitoh et al., 2014).

357   Decreases of ~1‰ in $\delta^{15}N$ values in late Permian Boreal and Panthalassic waters have also been
358   reported (Algeo et al., 2012; Grasby et al., 2015; Knies et al., 2013; Schoepfer et al., 2012). However,
359   with the exception of one study (Schoepfer et al., 2012), these changes are small and $\delta^{15}N$ values
360   never fall below +4‰. The persistence of positive $\delta^{15}N$ values indicate that these waters probably
361   maintained a robust NO_3^- inventory, which would have precluded an expansion in diazotrophy.

362 Small decreases in $\delta^{15}N$ values in LPEE sediments could be caused by several other factors. As
363 described above, differing rates of organic matter degradation tied to redox changes can influence the
364 $\delta^{15}N$ values of organic matter during deposition, particularly where fluxes of organic matter are low
365 (Freudenthal et al., 2001; Möbius et al., 2010). Such effects are illustrated by LPEE data from
366 Schuchert Dal, East Greenland (Mettam et al., 2017). C/N ratios in these sediments never exceed 6,
367 indicating little variation in organic matter provenance (e.g., due to terrestrial input). However, higher
368 $\delta^{15}N$ values and lower C/N ratios correspond with oxic, bioturbated depositional horizons, while
369 lower $\delta^{15}N$ values and higher C/N ratios are recorded in oxygen deficient, laminated horizons. Given
370 these observations, a wholesale transition from oxic to anoxic conditions during the LPEE coupled
371 with slower syn-depositional degradation could also contribute to decreases in $\delta^{15}N$ values at some
372 sites during and after the LPEE.

373 The complexity of interpreting sedimentary nitrogen isotope values is further highlighted by $\delta^{15}N$ data
374 from Buchanan Lake, Canada, which was part of the Sverdrup Basin on the northwest margin of
375 Pangea during the LPEE (Knies et al., 2013). These authors concluded that increased diazotrophy was
376 likely responsible for a small decrease in $\delta^{15}N$ (from ~+9‰ to ~+8‰) in these sediments. However,
377 persistently positive $\delta^{15}N$ values throughout this section suggest continued nitrate availability despite
378 evidence for an intensification of anoxia. A fall in the rate of organic matter degradation associated
379 with enhanced anoxia could be responsible for the small fall in $\delta^{15}N$; however, this scenario is
380 inconsistent with a coeval decrease in C/N ratios. An alternate explanation could come from increased
381 weathering and transport of exposed soils and terrestrial vegetation, consistent with the
382 reorganisation of terrestrial ecosystems during the LPEE (Algeo and Twitchett, 2010; Looy et al.,
383 2001). Increased fluxes of terrestrial organic matter are unlikely to be the cause of the decrease in
384 $\delta^{15}N$, as this would most likely increase C/N ratios as well. Alternatively, increased fluxes of clay-
385 adsorbed inorganic nitrogen from the depositional hinterland could change $\delta^{15}N$ whilst reducing C/N
386 ratios, as seen at this site. Given these alternative arguments, an increase in marine diazotrophy is a
387 reasonable, although perhaps not completely unique, interpretation.

388   **5. Future Perspectives**

389 These case studies highlight the potential complexity of the sedimentary $\delta^{15}N$ record and some of the
390 uncertainties associated with interpreting $\delta^{15}N$ values in deep time. In particular, the paucity of well-
391 preserved Archean sediments and inherent analytical limitations mean that the majority of $\delta^{15}N$
392 studies have focused on organic carbon-rich sediments deposited in low energy, deeper water settings.
393 These studies provide important constraints on local nitrogen cycling processes occurring in these
394 basins. However, the spatial heterogeneity of the marine N cycle, along with the ability of disparate N
395 cycling processes to produce overlapping $\delta^{15}N$ values, suggests that depositional and redox context is
396 critical in interpreting the resulting $\delta^{15}N$ records, and in unravelling local versus global signals. The
397 interpretation of Phanerozoic $\delta^{15}N$ records should similarly be approached with caution given the
398 multiple factors that can modify or overprint the isotopic characteristics of primary marine organic
399 matter. For example, redox variations can also influence organic matter degradation rates in the
400 sediments. Furthermore, the evolution of land plants during the Palaeozoic provide a source of
401 organic matter with distinct $\delta^{15}N$ values and C/N ratios, and the transport of these materials to the
402 sediments, along with nitrogen in eroded soils, can lead to mixing of isotope signals that complicate
403 interpretations. Additional targets for future and ongoing development include:

404 1. *Analytical advancements* – New methods are being developed to characterize the distribution of
405 $\delta^{15}N$ values in low N abundance sediments and to identify post-depositional alteration. In particular,
406 recent advances in *in situ* $\delta^{15}N$ analyses via SIMS will allow for direct analyses of $\delta^{15}N$ in organic
407 nitrogen (Ishida et al., 2018), which should allow for single-cell $\delta^{15}N$ analyses in Precambrian
408 microfossils.

409   2. *Field studies* – Modern anoxic aqueous environments, such as redox-stratified lakes and seas, can
410   provide near analogues to Precambrian marine systems. Thus $\delta^{15}N$ values of aqueous and sedimentary
411   N compounds in these systems can be linked directly to N cycling processes, providing important
412   insights into sedimentary $\delta^{15}N$ values preserved in ancient sediments (e.g., Fulton et al., 2018).

413   3. *Laboratory studies* – N isotopic fractionations produced during cyanobacterial N_2 fixation and
414   denitrification are generally well calibrated for modern conditions (Baursachs et al., 2009; Granger et
415   al., 2008), but life and environments have evolved significantly over Earth history. Past conditions
416   could have promoted different N cycling processes, by different groups of organisms and/or the same
417   organisms utilizing different enzymes, but the resulting isotopic fractionations are largely
418   unconstrained (e.g., Nishizawa et al., 2014). Incomplete ammonium assimilation in particular has
419   been implicated in contributing to Late Archean $\delta^{15}N$ records, but our understanding of $\delta^{15}N$
420   fractionations during this process, and their response to changing environmental conditions are
421   extremely limited (Hoch et al., 1992).

422   Combined, these types of inter-disciplinary studies could make the forward strides necessary for
423   generating and understanding sedimentary $\delta^{15}N$ records throughout Earth history.

424

425   **6. References (key references in bold)**

426   **Ader, M., Thomazo, C., Sansjofre, P., Busigny, V., Papineau, D., Laffont, R., Cartigny, P., and**
427   **Halverson, G. P., 2016, Interpretation of the nitrogen isotopic composition of**
428   **Precambrian sedimentary rocks: Assumptions and perspectives: Chemical Geology, v.**
429   **429, p. 93-110.**
430   Algeo, T., Henderson, C. M., Ellwood, B., Rowe, H., Elswick, E., Bates, S., Lyons, T., Hower, J. C.,
431   Smith, C., Maynard, B., Hays, L. E., Summons, R. E., Fulton, J. M., and Freeman, K. H.,
432   2012, Evidence for a diachronous Late Permian marine crisis from the Canadian Arctic
433   region: GSA Bulletin, v. 124, p. 1424-1448.
434   Algeo, T. J., and Twitchett, R. J., 2010, Anomalous Early Triassic sediment fluxes due to elevated
435   weathering rates and their biological consequences: Geology, v. 38, p. 1023-1026.
436   Altabet, M. A., and Francois, R., 1994, Sedimentary nitrogen isotopic ratio as a recorder for surface
437   ocean nitrate utilization: Global Biogeochemical Cycles, v. 8, no. 1, p. 103-116.
438   Bahlmann, E., Bernasconi, S. M., Bouillon, S., Houtekamer, M, Korntheuer, M., Langenberg, F.,
439   Mayr, C., Metzke, M., Middelburg, J. J., Nagel, B., Struck, U., Voss, M., and Emeis, K. C.,
440   2010, Performance evaluation of nitrogen isotope ratio determination in marine and lacustrine
441   sediments: an inter-laboratory comparison: Organic Geochemistry, v. 41, p. 3-12.
442   Baursachs, T., Schouten, S., Compaore, J., Wollenzien, U., Stal, L. J., and Damste, J. S. S., 2009,
443   Nitrogen isotopic fractionation associated with growth on dinitrogen gas and nitrate by
444   cyanobacteria: Limnology and Oceanography, v. 54, p. 1403-1411.
445   Beaumont, V., Agrinier, P., Javoy, M., and Robert, F., 1994, Determination of the CO contribution to
446   the 15N/14N ratio measured by mass spectrometry: Analytical Chemistry, v. 66, p. 2187-
447   2189.
448   **Beaumont, V., and Robert, F., 1999, Nitrogen isotope ratios of kerogens in Precambrian cherts:**
449   **a record of the evolution of atmosphere chemistry?: Precambrian Research, v. 96, p. 63-**
450   **82.**
451   Bebout, G. E., and Fogel, M. L., 1992, Nitrogen-isotope compositions of metasedimentary rocks in
452   the Catalina Schist, California - implications for metamorphic devolatilization history:
453   Geochimica et Cosmochimica Acta, v. 56, no. 7, p. 2839-2849.
454   Boyd, S. R., and Philippot, P., 1998, Precambrian ammonium biogeochemistry: a study of the Moine
455   metasediments, Scotland: Chemical Geology, v. 144, p. 257-268.
456   Brunner, B., Contreras, S., Lehmann, M. F., Matantseva, O., Rollog, M., Kalvelage, T., Klockgether,
457   G., Lavik, G., Jetten, M. S. M., Kartal, B., and Kuypers, M. M. M., 2013, Nitrogen isotope

458   effects induced by anammox bacteria: Proceedings of the National Academy of Sciences, v.
459   110, no. 47, p. 18994-18999.
460   **Busigny, V., Lebeau, O., Ader, M., Krapez, B., and Bekker, A., 2013, Nitrogen cycle in the Late**
461   **Archean ferruginous ocean: Chemical Geology, v. 362, p. 115-130.**
462   De Pol-Holz, R., Robinson, R. S., Hebbeln, D., Sigman, D. M., and Ulloa, O., 2009, Controls on
463   sedimentary nitrogen isotopes along the Chile margin: Deep-Sea Research Part Ii-Topical
464   Studies in Oceanography, v. 56, no. 16, p. 1100-1112.
465   Freudenthal, T., Wagner, T., Wenzhofer, F., Zabel, M., and Wefer, G., 2001, Early diagenesis of
466   organic matter from sediments of the eastern subtropical Atlantic: Evidence from stable
467   nitrogen and carbon isotopes: Geochimica et Cosmochimica Acta, v. 65, no. 11, p. 1795-
468   1808.
469   Fulton, J. M., Arthur, M. A., Thomas, B., and Freeman, K. H., 2018, Pigment carbon and nitrogen
470   isotopic signatures in euxinic basins: Geobiology, v. 16, p. 429-445.
471   Gao, X., Yang, Y., and Wang, C., 2012, Geochemistry of organic carbon and nitrogen in surface
472   sediments of coastal Bohai Bay inferred from their ratios and stable isotopic signatures:
473   Marine Pollution Bulletin, v. 64, p. 1148-1155.
474   Garvin, J., Buick, R., Anbar, A. D., Arnold, G. L., and Kaufman, A. J., 2009, Isotopic evidence for an
475   aerobic nitrogen cycle in the latest Archean: Science, v. 323, p. 1045-1048.
476   Godfrey, L. V., and Falkowski, P. G., 2009, The cycling and redox state of nitrogen in the Archaean
477   ocean: Nature Geoscience.
478   Granger, J., Sigman, D. M., Lehmann, M. F., and Tortell, P. D., 2008, Nitrogen and oxygen isotope
479   fractionation during dissimilatory nitrate reduction by denitrifying bacteria: Limnology and
480   Oceanography, v. 53, no. 6, p. 2533-2545.
481   Grasby, S., Beauchamp, B., Bond, D. P. G., Wignall, P. B., Talavera, C., Galloway, J. M., Piepjohn,
482   K., Reinhardt, L., and Blomeier, D., 2015, Progressive environmental deterioration in
483   northwestern Pangea leading to the latest Permian Extinction: GSA Bulletin, v. 127, p. 1331-
484   1347.
485   Hoch, M. P., Fogel, M. L., and Kirchman, D. L., 1992, Isotope fractionation associated with
486   ammonium uptake by a marine bacterium: Limnology and Oceanography, v. 37, no. 7, p.
487   1447-1459.
488   Ishida, A., Kitajima, K., Williford, K. H., Tuite, M. L., Kakegawa, T., and Valley, J. W., 2018,
489   Simultaneous in situ analysis of carbon and nitrogen isotope ratios in organic matter by
490   secondary ion mass spectrometry: Geostandards and Geoanalytical Research, p. 1-15.
491   Junium, C. K., and Arthur, M. A., 2007, Nitrogen cycling during the cretaceous, Cenomanian-
492   Turonian oceanic anoxic event II: Geochemistry Geophysics Geosystems, v. 8.
493   **Kipp, M. A., Stueken, E. E., Yun, M., Bekker, A., and Buick, R., 2018, Pervasive aerobic**
494   **nitrogen cycling in the surface ocean across the Paleoproterozoic era: Earth and**
495   **Planetary Science Letters, v. 500, p. 117-126.**
496   Knies, J., Grasby, S., Beauchamp, B., and Schubert, C. J., 2013, Water mass denitrification during the
497   latest Permian extinction in the Sverdrup Basin, Arctic Canada: Geology, v. 41, p. 167-170.
498   Koehler, M. C., Buick, R., Kipp, M. A., Stueken, E. E., and Zaloumis, J., 2018, Transient surface
499   ocean oxygenation recorded in the ~2.66-Ga Jeerinah Formation, Australia: Proceedings of
500   the National Academy of Sciences, v. 2018, p. 1-6.
501   Kump, L. R., Junium, C. K., Arthur, M. A., Brasier, A., Fallick, A., Melezhik, V., Lepland, A., Crne,
502   A. E., and Luo, G., 2011, Isotopic evidence for massive oxidation of organic matter following
503   the Great Oxidation Event: Science, v. 334, p. 1694-1696.
504   Looy, C. V., Twitchett, R. J., Dilcher, D. L., Van Konijnenburg-Van Cittert, J. H. A., and Visscher,
505   H., 2001, Life in the end-Permian dead zone: PNAS, v. 98, p. 7879-7883.
506   Macko, S. A., and Estep, M. F., 1984, Microbial alteration of stable nitrogen and carbon isotopic
507   compositions of organic matter: Organic Geochemistry, v. 6, p. 787-790.
508   Mandernack, K. W., Mills, C. T., Johnson, C. A., Rahn, T., and Kinney, C., 2009, The d15N and
509   d18O values of N2O produced during the co-oxidation of ammonia by methanotrophic
510   bacteria: Chemical Geology, v. 267, p. 96-107.

511   Megonigal, J.P., Hines, M.E., Visscher, P.T., 2003. 8.08 - Anaerobic Metabolism: Linkages to Trace
512   Gases and Aerobic Processes. In: 'Treatise on Geochemistry' Holland and Turekian (eds.) p.
513   317-424.
514   Mettam, C., Zerkle, A. L., Claire, M. C., Izon, G., Junium, C. K., and Twitchett, R. J., 2017, High-
515   frequency fluctuations in redox conditions during the latest Permian mass extinction:
516   Palaeogeography Palaeoclimatology Palaeoecology, v. 485, p. 210-223.
517   Meyers, P. A., 1997, Organic geochemical proxies of paleoceanographic, paleolimnologic, and
518   paleoclimatic processes: Organic Geochemistry, v. 27, p. 213-250.
519   Möbius, J., Lahajnar, N., and Emeis, K. C., 2010, Diagenetic control of nitrogen isotope ratios in
520   Holocene sapropels and recent sediments from the Eastern Mediterranean Sea:
521   Biogeosciences Discussions, v. 7, p. 1131-1165.
522   Nishizawa, M., Miyazaki, J., Makabe, A., Koba, K., and Takai, K., 2014, Physiological and isotopic
523   characteristics of nitrogen fixation by hyperthermophilic methanogens: Key insights into
524   nitrogen anabolism of the microbial communities in Archean hydrothermal systems:
525   Geochimica et Cosmochimica Acta, v. 138, p. 117-135.
526   Olsen, S. L., Kump, L. R., and Kasting, J. F., 2013, Quantifying the areal extent and dissolved oxygen
527   concentrations of Archean oxygen oases: Chemical Geology, v. 362, p. 35-43.
528   Papineau, D., Mojzsis, S. J., Karhu, J. A., Marty, B., 2005, Nitrogen isotopic composition of
529   ammoniated phyllosilicates: case studies from Precambrian metamorphosed sedimentary
530   rocks: Chemical Geology, v. 216, p. 37-58.
531   Pinti, D. L., and Hashizume, K., 2011, Early Life Records from Nitrogen Isotopes, *in* Golding, S., and
532   Glikson, M., eds., Earliest life on Earth: Habitats, Environments, and Methods of Detection:
533   Dordrecht, Springer.Peters, K. E., Sweeney, R. E., and Kaplan, I. R., 1978, Correlation of
534   carbon and nitrogen stable isotope ratios in sedimentary organic matter: Limnology and
535   Oceanography, v. 23, p. 598-604.
536   Polissar, P. J., Fulton, J. M., Junium, C. K., Turich, C. H., and Freeman, K. H., 2009, Measurement of
537   13C and 15N isotopic composition on nanomolar quantitites of C and N: Analytical
538   Chemistry, v. 81, p. 755-763.
539   **Robinson, R. S., Kienast, M., Albuquerque, A. L., Altabet, M., Contreras, S., De Pol Holz, R.,**
540   **Dubois, N., Francois, R., Galbraith, E., Hsu, T.-C., Ivanochko, T., Jaccard, S., Kao, S.-**
541   **J., Kiefer, T., Kienast, S., Lehmann, M. F., Martinez, P., McCarthy, M., Moebius, J.,**
542   **Pedersen, T., Quan, T. M., Ryabenko, E., Schmittner, A., Schneider, R., Schneider-Mor,**
543   **A., Shigemitsu, M., Sinclair, D., Somes, C., Studer, A., Thunell, R., and Yang, J.-Y.,**
544   **2012, A review of nitrogen isotopic alteration in marine sediments: Paleoceanography, v.**
545   **27.**
546   Saitoh, M., Ueno, Y., Nishizawa, M., Isozaki, Y., Takai, K., Yao, J., and Ji, Z., 2014, Nitrogen isotope
547   chemostratigraphy across the Permian-Triassic boundary at Chaotian, Sichuan, South China:
548   Journal of Asian Earth Sciences, v. 93, p. 113-128.
549   Schoepfer, S. D., Henderson, C. M., Garrison, G. H., and Ward, P. D., 2012, Cessation of a
550   productive coastal upwelling system in the Panthalassic Ocean at the Permian-Triassic
551   boundary: Palaeogeography Palaeoclimatology Palaeoecology, v. 313, p. 181-188.
552   Stüeken, E. E., Buick, R., Guy, B., and Koehler, M. C., 2015a, Isotopic evidence for biological
553   nitrogen fixation by Mo-nitrogenase from 3.2 Gyr: Nature, v. 520, p. 666-669.
554   Stüeken, E. E., Buick, R., and Schauer, A. J., 2015b, Nitrogen isotope evidence for alkaline lakes on
555   late Archean continents: Earth and Planetary Science Letters, v. 411, p. 1-10.
556   **Stüeken, E. E., Kipp, M. A., Koehler, M. C., and Buick, R., 2016a, The evolution of Earth's**
557   **biogeochemical nitrogen cycle: Earth-Science Reviews, v. 160, p. 220-239.**
558   Stüeken, E. E., Zaloumis, J., Meixnerova, J., and Buick, R., 2017, Differential metamorphic effects on
559   nitrogen isotopes in kerogen extracts and bulk rocks: Geochimica et Cosmochimica Acta, v.
560   217, p. 80-94.
561   Thomazo, C., Ader, M., and Philippot, P., 2011, Extreme 15N-enrichments in 2.72-Gyr-old
562   sediments: evidence for a turning point in the nitrogen cycle: Geobiology, v. 9, no. 2, p. 107-
563   120.

13

564 Voss, M., Bange, H. W., Dippner, J. W., Middelburg, J. J., , Montoya, J. P., Ward, B., 2013, The
565   marine nitrogen cycle: recent discoveries, uncertainties and the potential relevance of climate
566   change. Philosophical Transactions Royal Society of London B Biological Science. v. 368.
567 Weiss, M. C., Sousa, F. L., N., M., Neukirchen, S., Roettger, M., Nelson-Sathi, S., and Martine, W.
568   F., 2016, The physiology and habitat of the last universal common ancestor: Nature
569   Microbiology, v. 1, p. 16116.
570 Yang, J., Junium, C. K., Grassineau, N. V., Nisbet, E. G., Izon, G., Mettam, C., Martin, A., and
571   Zerkle, A. L., 2019, Ammonium availability in the Late Archaean nitrogen cycle: Nature
572   Geoscience, v. 12, no. 7, p. 553-557.
573 Zerkle, A. L., House, C. H., Cox, R. P., and Canfield, D. E., 2006, Metal limitation of cyanobacterial
574   N_2 fixation and implications for the Precambrian nitrogen cycle: Geobiology, v. 4, p. 285-
575   297.**Zerkle, A. L., Poulton, S. W., Newton, R. J., Mettam, C., Claire, M. W., Bekker, A.,
576   and Junium, C. K., 2017, Onset of the aerobic nitrogen cycle during the Great Oxidation
577   Event: Nature, v. 542, p. 465-467.**